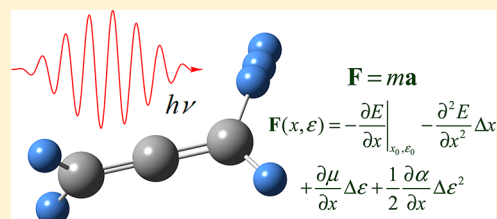


Molecular Dynamics in Strong Laser Fields: A New Algorithm for ab Initio Classical Trajectories

H. Bernhard Schlegel*

Department of Chemistry, Wayne State University, Detroit, Michigan 48202, United States

ABSTRACT: A new, more accurate Hessian-based predictor-corrector algorithm has been developed for simulating classical trajectories of molecules in intense laser fields. The first and second derivatives of the gradient with respect to the electric field are included in the both the predictor and the corrector steps for integrating trajectories. A Taylor expansion of the gradient is used as the surface for integrating the predictor step; a distance weighted interpolant of the gradient is employed for the corrector step. Test trajectories were calculated for HCO^+ in a continuous $10 \mu\text{m}$, $2.9 \times 10^{14} \text{ W cm}^{-2}$ laser field and triplet allene dication in a $10 \mu\text{m}$, $5.7 \times 10^{13} \text{ W cm}^{-2}$ four cycle cosine pulse. The first derivative of the gradient with respect to the electric field makes a significant contribution, while the second derivative makes a smaller contribution and can be neglected. To reduce the cost, the Hessian can be updated for several steps before being recalculated. The calculations indicate that a step size of $\Delta t = 0.25 \text{ fs}$ and 20 updates is efficient and reliable for these test systems.



INTRODUCTION

Short, intense laser pulses can deposit a substantial amount of energy in a molecule. Such highly energized molecules can undergo rapid rearrangements and dissociation (for some leading references, see refs 1–10 and references therein). For intensities in the range of $10^{14} \text{ W cm}^{-2}$, the electric field can distort the potential energy surface significantly. At optical frequencies, the electric field oscillates rapidly compared to the molecular motion. As a result, the motion of a molecule responds primarily to the cycle-averaged influence of the field on the potential energy surface. However, at infrared frequencies, the oscillation of the electric field is on the same time scale as the nuclear motion. Strong fields can cause extensive changes in the charge distribution and alter barriers substantially. Consequently, the dynamics are affected by the instantaneous field strength. In particular, this can result in rapid dissociation and highly energized fragments. Calculations indicate that if the molecule can be aligned in the field, very short and intense mid-IR pulses can cause the selective dissociation of stronger bonds in CF_3Br^+ and $\text{C}_6\text{H}_5\text{I}^{2+}$ ¹¹ and can enhance the yield of higher energy HCl^+ products in the fragmentation of formyl chloride cation, ClCHO^+ .¹²

The effect of a strong electric field on the motion of a molecule can be simulated by ab initio molecular dynamics (AIMD) calculations^{13–15} in the time-varying field. In AIMD calculations, an electronic structure computation is carried out each time the forces on the atoms in a molecule are needed to integrate the classical equations of motion. Numerous algorithms are available to integrate classical equations of motion for molecular systems.¹⁶ The aim of a good AIMD algorithm is to minimize the cost by reducing the number of electronic structure computations, but without sacrificing accuracy of the trajectory calculation. Methods such as velocity Verlet, fourth-order Runge–Kutta, and Adams–Bashforth–

Moulton require only gradients from the electronic structure calculations.¹⁷ However, the step size must be relatively small in order to maintain good accuracy. If the Hessian or second derivative matrix can be calculated, significantly large steps can be taken, but at the cost of a more expensive electronic structure calculation.¹⁸ Predictor-corrector methods using Hessians allow for larger step sizes without a loss of accuracy.^{19,20} The overall cost of the electronic structure calculations can be reduced by updating the Hessian for five to 10 steps before recalculating it analytically.²¹ Specialized updating methods have been developed for updating Hessians during trajectory calculation.²²

In the field-free case, our Hessian-based predictor-corrector (HPC) method with updating^{20,21} is up to 30 times more efficient than velocity Verlet for molecules with up to 12 heavy atoms. A predictor step is taken on a local quadratic surface obtained from a Hessian calculation. A fifth order polynomial surface is fitted to the calculated energy, gradient, and Hessian at the beginning and end of the predictor step and is used to calculate a corrector step. The Hessian can be updated for up to 10 steps before being recalculated analytically. By calculating the gradient and Hessian in the instantaneous field, this method can be used for the dynamics of molecules in oscillating fields, e.g. laser pulses. At mid-IR frequencies, we find that the step size must be limited to a small fraction of the period of the field, and the fitted energy surface must be restricted to a fourth order polynomial.²³ For intense fields and higher frequencies, the time-varying electric field should be included in the integration of both the predictor and corrector steps.

The present paper describes a new, more accurate Hessian-based predictor-corrector algorithm for simulating classical

Received: May 13, 2013

Published: June 25, 2013

trajectories of molecules in intense laser fields. The effect of the time-varying electric field on the potential energy surface is taken into account by including the first and second derivatives of the gradient with respect to the electric field. The potential energy surface of the corrector step is modeled with a distance weighted interpolant surface^{24–26} for the gradient. The present work was stimulated by the fact that distance weighted interpolants combined with trajectory integration methods are quite efficient for following steepest descent reaction paths.^{27–29}

METHOD

The potential energy surface of a molecule can be expanded as a Taylor series in terms of the position of the atoms and the applied electric field:

$$\begin{aligned}
 E(\vec{x}, \vec{e}(t)) &= E(\vec{x}_1, \vec{e}(t_1)) + \left. \frac{\partial E}{\partial \vec{x}} \right|_{\vec{x}_1, \vec{e}(t_1)} (\vec{x} - \vec{x}_1) \\
 &+ \frac{1}{2} \left. \frac{\partial^2 E}{\partial \vec{x}^2} \right|_{\vec{x}_1, \vec{e}(t_1)} (\vec{x} - \vec{x}_1)^2 + \left. \frac{\partial E}{\partial \vec{e}} \right|_{\vec{x}_1, \vec{e}(t_1)} (\vec{e}(t) - \vec{e}(t_1)) \\
 &+ \frac{1}{2} \left. \frac{\partial^2 E}{\partial \vec{e}^2} \right|_{\vec{x}_1, \vec{e}(t_1)} (\vec{e}(t) - \vec{e}(t_1))^2 \\
 &+ \left. \frac{\partial^2 E}{\partial \vec{x} \partial \vec{e}} \right|_{\vec{x}_1, \vec{e}(t_1)} (\vec{x} - \vec{x}_1)(\vec{e}(t) - \vec{e}(t_1)) \\
 &+ \frac{1}{2} \left. \frac{\partial^3 E}{\partial \vec{x} \partial \vec{e}^2} \right|_{\vec{x}_1, \vec{e}(t_1)} (\vec{x} - \vec{x}_1)(\vec{e}(t) - \vec{e}(t_1))^2 \\
 &+ \text{higher cross terms}
 \end{aligned} \quad (1)$$

The first and second derivatives with respect to the electric field correspond to the dipole moment and the polarizability. The first two mixed derivatives

$$\frac{\partial^2 E}{\partial \vec{e} \partial \vec{x}} = -\frac{\partial \vec{\mu}}{\partial \vec{x}} = \frac{\partial \vec{g}}{\partial \vec{e}} \quad \text{and} \quad \frac{\partial^3 E}{\partial \vec{e}^2 \partial \vec{x}} = -\frac{\partial \alpha}{\partial \vec{x}} = \frac{\partial^2 \vec{g}}{\partial \vec{e}^2} \quad (2)$$

are dipole and polarizability derivatives. In many electronic structure codes, these are computed together with the Hessian, since they are needed in vibrational frequency calculation for the infrared and Raman intensities. Higher mixed derivatives would include $\partial^3 E / \partial \vec{x}^2 \partial \vec{e}$, but these are often not available in typical vibrational frequency calculations.

The energy of a charged molecule in a uniform electric field depends on the position of the molecule in the field. However, the integration of a classical trajectory step requires only the gradients for internal motion of the molecule, and these do not depend on the translational position of the molecule in the uniform electric field. The Taylor expansion of the gradient is

$$\begin{aligned}
 \vec{g}(\vec{x}, \vec{e}(t)) &= \vec{g}(\vec{x}_1, \vec{e}(t_1)) + \left. \frac{\partial \vec{g}}{\partial \vec{x}} \right|_{\vec{x}_1, \vec{e}(t_1)} (\vec{x} - \vec{x}_1) \\
 &+ \left. \frac{\partial \vec{g}}{\partial \vec{e}} \right|_{\vec{x}_1, \vec{e}(t_1)} (\vec{e}(t) - \vec{e}(t_1)) \\
 &+ \frac{1}{2} \left. \frac{\partial^2 \vec{g}}{\partial \vec{e}^2} \right|_{\vec{x}_1, \vec{e}(t_1)} (\vec{e}(t) - \vec{e}(t_1))^2 \\
 &+ \text{higher terms}
 \end{aligned} \quad (3)$$

If the higher terms are dropped and no electric field is applied, this can be integrated analytically. If a time-varying field is included, the integration for a time step of Δt must be done numerically. In the present approach, the velocity Verlet method is used to integrate the predictor step on this surface using a small step size of δt . Tests indicate $\delta t = \Delta t/100$ yields an accurate integration for typical trajectories.

After an integration step of Δt on the surface given by eq 3, the energy derivatives can be recalculated and the process repeated for the next step of Δt . Alternatively, the integration using eq 3 can be considered a predictor step. A corrector step can then be taken on a surface fitted to the energy and derivatives calculated at the beginning and end of the predictor step. In our original implementation of this approach, we used a fifth order polynomial to fit the potential energy surface for trajectories without an electric field.^{19,20} For a charged molecule in an electric field, we had to reduce the polynomial to fourth order (dropping one of the energies²³) because the energy of a charged molecule depends on its position in the field. Alternatively, one can avoid this problem by fitting the gradient surface rather than the energy surface. A distance-weighted interpolant (DWI) or Shepard interpolation is a flexible and convenient form for the gradient surface. In a DWI, local descriptions of the surface are patched together using weights that are a function of the inverse distance.^{24–26}

$$\begin{aligned}
 \vec{g}(\vec{x}, \vec{e}(t)) &= w_1(\vec{x}) \vec{g}_1(\vec{x}, \vec{e}(t)) + w_2(\vec{x}) \vec{g}_2(\vec{x}, \vec{e}(t)) \\
 w_1(\vec{x}) &= 1/|\vec{x} - \vec{x}_1|^2 / (1/|\vec{x} - \vec{x}_1|^2 + 1/|\vec{x} - \vec{x}_2|^2) \\
 &= |\vec{x} - \vec{x}_2|^2 / (|\vec{x} - \vec{x}_1|^2 + |\vec{x} - \vec{x}_2|^2), \\
 w_2(\vec{x}) &= 1/|\vec{x} - \vec{x}_2|^2 / (1/|\vec{x} - \vec{x}_1|^2 + 1/|\vec{x} - \vec{x}_2|^2) \\
 &= |\vec{x} - \vec{x}_1|^2 / (|\vec{x} - \vec{x}_1|^2 + |\vec{x} - \vec{x}_2|^2)
 \end{aligned} \quad (4)$$

For the present two-point DWI, the inverse distance squared generates a sufficiently smooth interpolation surface. The local functions for the gradient used in the DWI

$$\begin{aligned}
 \vec{g}_n(\vec{x}, \vec{e}(t)) &= \vec{g}(\vec{x}_n, \vec{e}(t_n)) + \left. \frac{\partial \vec{g}}{\partial \vec{x}} \right|_{\vec{x}_n, \vec{e}(t_n)} (\vec{x} - \vec{x}_n) \\
 &+ \frac{1}{2} \left. \frac{\partial^2 \vec{g}}{\partial \vec{x}^2} \right|_{\vec{x}_n, \vec{e}(t_n)} (\vec{x} - \vec{x}_n)^2 + \left. \frac{\partial \vec{g}}{\partial \vec{e}} \right|_{\vec{x}_n, \vec{e}(t_n)} (\vec{e}(t) - \vec{e}(t_n)) \\
 &+ \frac{1}{2} \left. \frac{\partial^2 \vec{g}}{\partial \vec{e}^2} \right|_{\vec{x}_n, \vec{e}(t_n)} (\vec{e}(t) - \vec{e}(t_n))^2
 \end{aligned} \quad (5)$$

include third derivatives of the energy obtained by numerical differentiation of the Hessians.

$$\frac{\partial^2 \vec{g}}{\partial \vec{x}^2} = \frac{\partial^3 E}{\partial \vec{x}^3} \approx \left(\left. \frac{\partial^2 E}{\partial \vec{x}^2} \right|_{\vec{x}_2} - \left. \frac{\partial^2 E}{\partial \vec{x}^2} \right|_{\vec{x}_1} \right) / (\vec{x}_2 - \vec{x}_1) \quad (6)$$

Since the change in the trajectory due to the corrector step is small, the gradient, Hessian, dipole derivatives and polarizability derivatives calculated at \vec{x}_2 are used for the predictor phase of the next step. Thus, only one electronic structure calculation is required for each integration step.

As with our earlier Hessian-based predictor-corrector algorithms,^{19–21} the Hessian can be updated for a number of steps before it needs to be recalculated analytically. The Hessian updating formulas used in quasi-Newton based optimization methods yield Hessians that are appropriate for

the midpoint of the step from \vec{x}_1 to \vec{x}_2 . The compact finite difference (CFD) updating approach of Wu et al.²² uses the gradients \vec{g}_1 and \vec{g}_2 to update the Hessian at \vec{x}_1 to give a good estimate of the Hessian at \vec{x}_2 . The resulting update is twice the size of the conventional update. The CFD version of the Bofill update^{30,31} is used in the present work (i.e., twice the regular Bofill update).

Test calculations were carried out with the development version of the Gaussian series of electronic structure codes.³² AIMD calculations on HCO⁺ were carried out at the B3LYP/6-311G(d,p) level of theory using a continuous laser field with a wavelength of $\lambda = 10 \mu\text{m}$ ($\omega = 0.188 \text{ fs}^{-1}$) and an intensity of $2.9 \times 10^{14} \text{ W cm}^{-2}$ (0.09 au). Calculations for H₂CCCH₂²⁺ were carried out at the B3LYP/6-31G(d,p) level of theory using a four cycle cosine pulse with a wavelength of $\lambda = 10 \mu\text{m}$ and maximum intensity of $5.7 \times 10^{13} \text{ W cm}^{-2}$ (0.04 au).

TESTS

Energy conservation is often used as a test for the accuracy of a classical trajectory integration algorithm. A molecule in an oscillating electric field will gain energy from the field. Hence, an alternative test is needed to assess the accuracy of a trajectory calculation for a molecule in a strong laser field. A rather stringent test is to compare the time evolution of the positions of the atoms in a molecule to an accurate reference trajectory. In a previous study, we examined the dissociation of HCO⁺ aligned in a laser field.²³ The variation of the C–H bond length for a selected trajectory is shown in Figure 1. The laser

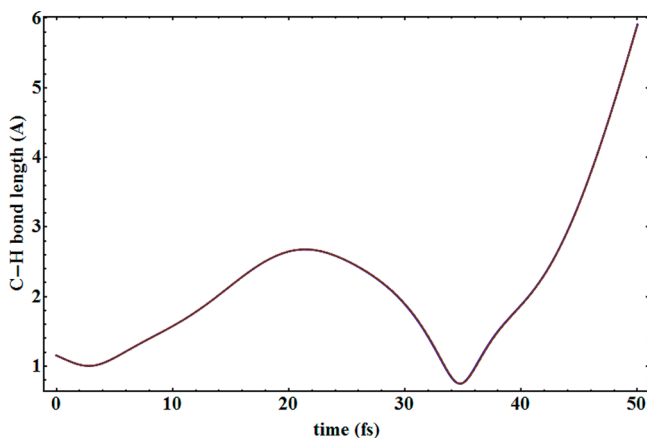


Figure 1. A dissociative trajectory of HCO⁺ in a continuous laser field ($10 \mu\text{m}$, $2.9 \times 10^{14} \text{ W cm}^{-2}$, aligned with the molecular axis). Trajectories for $\Delta t = 0.05, 0.10, 0.25,$ and 0.50 fs are indistinguishable on this scale.

field ($10 \mu\text{m}$, $2.9 \times 10^{14} \text{ W cm}^{-2}$, aligned with the molecular axis) first stretches the C–H bond and then compresses it; after the inner turning point, the field suppresses the bond dissociation barrier and accelerates the H⁺ to dissociation. The time of the inner turning point of this trajectory is a convenient landmark for the comparison of integration methods.

A reference trajectory has been calculated using eq 3 with decreasing step sizes. With step sizes of $\Delta t = 0.100, 0.050,$ and 0.025 fs , the times for the inner turning point of the trajectory are 35.74, 35.26, and 35.02, respectively, and extrapolate linearly to a limit of $t = 34.78 \text{ fs}$. Using the same starting conditions, trajectories calculated with our older Hessian-based predictor-corrector method also converge to the same limit for

the inner turning point.²³ With the present Hessian-based predictor-corrector method using dipole and polarizability derivatives in eqs 3–5 without Hessian updating using step sizes of $\Delta t = 0.50, 0.25, 0.10,$ and 0.05 fs , the inner turning point occurs at 34.75, 34.76, 34.77, and 34.77 fs, respectively. The trajectory with $\Delta t = 0.05 \text{ fs}$ is used as the reference trajectory in Figures 2–4.

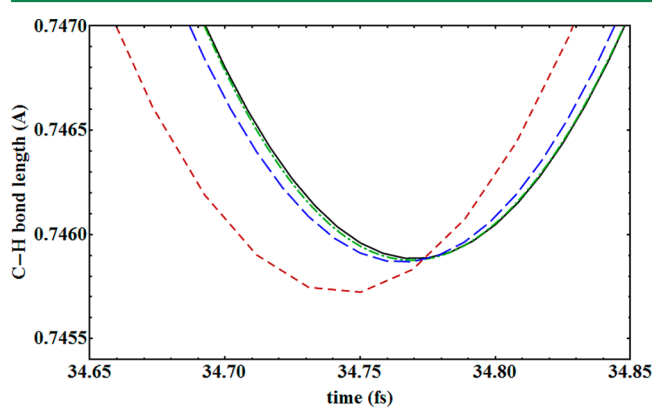


Figure 2. Close-up of the inner turning point region in Figure 1 showing the convergence of trajectories with step size without Hessian updating: $\Delta t = 0.05, 0.10, 0.25,$ and 0.50 fs in solid black, dot-dash green, long dash blue, and short dash red, respectively.

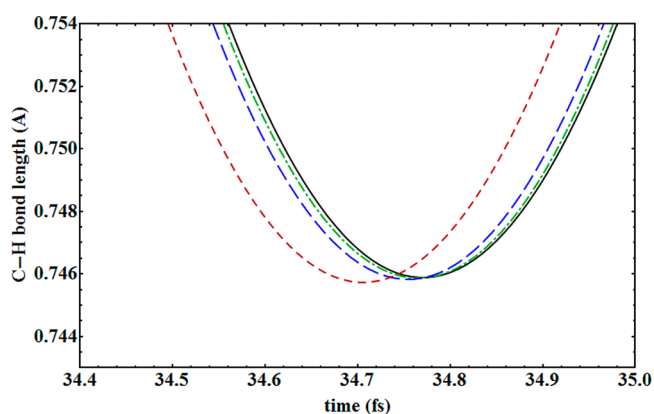


Figure 3. Close-up of the inner turning point region in Figure 1 showing the effect of including the dipole and polarizability derivatives in the trajectory integration: reference trajectory with step size $\Delta t = 0.05 \text{ fs}$ and using dipole and polarizability derivatives (solid, black); test trajectories (step size $\Delta t = 0.25 \text{ fs}$) with dipole and polarizability derivatives (dot-dash, green), with dipole derivative but no polarizability derivative (long dash, blue), and without dipole and polarizability derivatives (short dash, red).

On the scale of Figure 1, trajectories for $\Delta t = 0.05, 0.10, 0.25,$ and 0.50 fs are superimposable and indistinguishable. Figure 2 shows interpolated trajectories for a very small section near the inner turning point appearing in Figure 1. The trajectories without updating are essentially converged with step sizes of $\Delta t = 0.10$ and 0.25 fs . With $\Delta t = 0.50 \text{ fs}$, the inner turning point is within 0.02 fs of the reference trajectory. Thus, without updating, step sizes up to 0.50 fs could be used for HCO⁺ without any significant loss of accuracy.

The effect of including the dipole and polarizability terms in the present Hessian-based predictor-corrector method is illustrated in Figure 3. The trajectory with step size $\Delta t = 0.25 \text{ fs}$ and using both the dipole and polarizability derivatives is

nearly the same as the reference trajectory with $\Delta t = 0.05$ fs. If the polarizability contribution is dropped from eqs 3–5, the

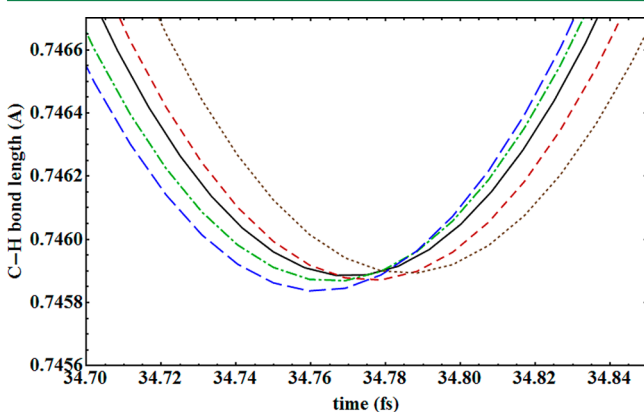


Figure 4. Close-up of the inner turning point region in Figure 1 showing the effect of updating on the trajectory integration: reference trajectory with step size $\Delta t = 0.05$ fs and no updating (solid, black); test trajectories (step size $\Delta t = 0.25$ fs) with no updating (dot-dash, green), and with updating for 10 steps (long dash, blue), 20 steps (short dash, red), and 30 steps (dot, brown).

inner turning point is within 0.02 fs of the reference trajectory. However, if both the dipole and polarizability terms are dropped, the error is ca. 0.07 fs. Thus, the dipole term makes an important contribution and needs to be included. The polarizability term makes only a small contribution at these very high field strengths (0.09 au) and need not be included. The polarizability contribution should become even less important at lower, more reasonable field strengths.

Figure 4 shows the effect of updating the Hessian for $n - 1$ steps and recalculating the full Hessian every n th step. For a step size of $\Delta t = 0.25$ fs, the errors in the turning point are 0.00, 0.01, and 0.03 fs for $n = 10, 20,$ and 30 compared to the reference trajectory with $n = 0$. Thus, it is safe to update the Hessian and recalculate it only every 20th or 30th step. Since the cost of a Hessian calculation is typically 8–10 times the cost of a gradient calculation for molecules with four to eight heavy atoms, a trajectory with updating for 20 steps is ca. 1/6 of the cost of a trajectory without updating but has nearly the same accuracy. Results for other combinations of step size and updating are listed in Table 1. A larger step size of $\Delta t = 0.50$ fs

Table 1. Interpolated Times for the Inner Turning Point of a HCO^+ Trajectory As a Function of the Step Size and Number of Updates

Δt (fs)	$n = 0$	$n = 10$	$n = 20$	$n = 30$
0.05	34.77			
0.10	34.77	34.77	34.77	
0.25	34.76	34.76	34.77	34.79
0.50	34.75	34.81	34.87	34.93

is possible for this system, but the cost is about the same because the Hessian needs to be recalculated more frequently to maintain the same accuracy. A good compromise between accuracy, reliability, and efficiency for systems and conditions similar to the HCO^+ test case seems to be $\Delta t = 0.25$ fs and $n = 20$.

The dissociation of energized allene dication, $\text{H}_2\text{CCCH}_2^{2+}$, has been studied previously by classical trajectory methods.³³

Triplet allene dication was chosen as a second test case. Trajectories were calculated for a four cycle cosine pulse with a wavelength of $10 \mu\text{m}$ and a maximum intensity of $5.7 \times 10^{13} \text{ W cm}^{-2}$ aligned with the CCC bond. These conditions were chosen so that allene would dissociate late in the pulse or shortly after the pulse. Allene was given zero point energy with the phases of the vibrations chosen randomly and no rotational energy. The trajectories were integrated for 300 fs (i.e., 133.7 fs within the pulse and 166.3 fs field-free after the pulse) with the new Hessian-based predictor-corrector method using the dipole derivatives but not the polarizability derivatives. A small test set of 10 trajectories yielded three with C–H dissociation during the pulse, three with C–H dissociation after the pulse, one trajectory with a few 1,2 hydrogen shifts, two with a combination of 1,2 hydrogen shifts and C–H dissociation, and two trajectories with no reaction. This is consistent with earlier calculations^{33,34} that found the lowest barriers on the triplet dication surface were 43 kcal/mol for 1,2 hydrogen shift and 60 kcal/mol for C–H dissociation. From this set, one of the trajectories with C–H dissociation after the pulse was chosen to test the new trajectory integration method. Table 2

Table 2. Dissociation Times^a for a $\text{H}_2\text{CCCH}_2^{2+}$ Trajectory As a Function of the Step Size and Number of Updates

Δt (fs)	$n = 0$	$n = 10$	$n = 20$	$n = 30$
0.05	155.13			
0.10	155.05	155.07	155.07	155.05
0.25	154.82	154.83	154.77	154.72
0.50	154.53	154.16	154.29	153.77

^aTime required for a C–H bond to reach 5 Å.

lists the times for C–H bond dissociation as a function of the step size and number of updates. The dissociation time is taken as the time needed for the C–H bond to reach 5.00 Å. Extrapolating the data in the column with no updates ($n = 0$) yields a dissociation time of 155.21 fs. The trajectory with step sizes of $\Delta t = 0.10, 0.25,$ and 0.50 fs trajectories have errors of 0.16, 0.39, and 0.68 fs in the dissociation time. Updating the Hessian and recalculating it every 10, 20, or 30 steps ($n = 10, 20, 30$) has almost no effect on the dissociation time for trajectories with a step size of $\Delta t = 0.10$ fs. The errors in the C–H dissociation times for $\Delta t = 0.25$ fs are only 0.01, 0.05, and 0.10 fs for updating the Hessian for $n = 10, 20,$ and 30 , respectively, compared to $n = 0$. For a step size of $\Delta t = 0.50$ fs, the errors in the dissociation time due to updating become somewhat larger. As in the case of HCO^+ , the data suggest that a step size of $\Delta t = 0.25$ fs and 20 updates yields an efficient and reliable integration of the classical trajectories for triplet allene dication under the present conditions.

SUMMARY

This paper describes a new, more accurate Hessian-based predictor-corrector algorithm that can calculate classical trajectories of molecules in intense laser fields as efficiently as under field-free conditions. In addition to the first and second derivatives of the energy with respect to the nuclear coordinates, this method also uses the first and second derivatives of the gradient with respect to the electric field (i.e., the dipole and polarizability derivatives). Using the velocity Verlet algorithm, a predictor step is taken using a Taylor expansion of the gradient; a corrector step is integrated on a distance weighted interpolant of the gradient using Taylor

expansions of the gradient at the beginning and end of the predictor step. Test were carried out for HCO^+ in a continuous $10 \mu\text{m}$, $2.9 \times 10^{14} \text{ W cm}^{-2}$ laser field and triplet allene dication in a $10 \mu\text{m}$, $5.7 \times 10^{13} \text{ W cm}^{-2}$ 4 cycle cosine pulse. The dipole derivatives make an important contribution, but the polarizability derivatives make a smaller contribution and need not be included even for fields as large as $3 \times 10^{14} \text{ W cm}^{-2}$. Updating the Hessian a number of steps before recalculating it can reduce the cost of a trajectory by a substantial factor. The calculations indicate that a step size of $\Delta t = 0.25 \text{ fs}$ and 20 updates is efficient and reliable for these test systems.

AUTHOR INFORMATION

Corresponding Author

*E-mail: hbs@chem.wayne.edu.

Notes

The authors declare no competing financial interest.

ACKNOWLEDGMENTS

This work was supported by a grant from the National Science Foundation (CHE1212281). Wayne State University's computing grid provided computational support.

REFERENCES

- (1) Chelkowski, S.; Bandrauk, A. D.; Corkum, P. B. Efficient molecular dissociation by a chirped ultrashort infrared-laser pulse. *Phys. Rev. Lett.* **1990**, *65*, 2355–2358.
- (2) Conjusteau, A.; Bandrauk, A. D.; Corkum, P. B. Barrier suppression in high intensity photodissociation of diatomics: Electronic and permanent dipole moment effects. *J. Chem. Phys.* **1997**, *106*, 9095–9104.
- (3) Hishikawa, A.; Hasegawa, H.; Yamanouchi, K. Hydrogen migration in acetonitrile in intense laser fields in competition with two-body Coulomb explosion. *J. Electron. Spectrosc.* **2004**, *141*, 195–200.
- (4) Hertel, I. V.; Radloff, W. Ultrafast dynamics in isolated molecules and molecular clusters. *Rep. Prog. Phys.* **2006**, *69*, 1897–2003.
- (5) Itakura, R.; Liu, P.; Furukawa, Y.; Okino, T.; Yamanouchi, K.; Nakano, H. Two-body Coulomb explosion and hydrogen migration in methanol induced by intense 7 and 21 fs laser pulses. *J. Chem. Phys.* **2007**, *127*, 104306.
- (6) Xu, H.; Okino, T.; Yamanouchi, K. Tracing ultrafast hydrogen migration in allene in intense laser fields by triple-ion coincidence momentum imaging. *J. Chem. Phys.* **2009**, *131*, 151102.
- (7) Xu, H.; Okino, T.; Nakai, K.; Yamanouchi, K.; Roither, S.; Xie, X.; Kartashov, D.; Zhang, L.; Baltuska, A.; Kitzler, M. Two-proton migration in 1,3-butadiene in intense laser fields. *Phys. Chem. Chem. Phys.* **2010**, *12*, 12939–12942.
- (8) Xu, H.; Okino, T.; Yamanouchi, K. Ultrafast delocalization of hydrogen atoms in allene in intense laser fields. *Appl. Phys. A: Mater. Sci. Process.* **2011**, *104*, 941–945.
- (9) Okino, T.; Watanabe, A.; Xu, H.; Yamanouchi, K. Ultrafast hydrogen scrambling in methylacetylene and methyl-d(3)-acetylene ions induced by intense laser fields. *Phys. Chem. Chem. Phys.* **2012**, *14*, 10640–10646.
- (10) Geissler, D.; Marquetand, P.; Gonzalez-Vazquez, J.; Gonzalez, L.; Rozgonyi, T.; Weinacht, T. Control of nuclear dynamics with strong ultrashort laser pulses. *J. Phys. Chem. A* **2012**, *116*, 11434–11440.
- (11) Lee, S. K.; Schlegel, H. B.; Li, W. Bond selective dissociation of polyatomic ions in mid-infrared strong fields. *J. Phys. Chem. A*. Submitted.
- (12) Lee, S. K.; Suits, A. G.; Schlegel, H. B.; Li, W. A reaction accelerator: Mid-infrared strong field dissociation yields mode-selective chemistry. *J. Phys. Chem. Lett.* **2012**, *3*, 2541–2547.
- (13) Bolton, K.; Hase, W. L.; Peslherbe, G. H. Direct dynamics of reactive systems. In *Modern Methods for Multidimensional Dynamics Computation in Chemistry*; Thompson, D. L., Ed.; World Scientific: Singapore, 1998; pp 143–189.
- (14) Sun, L. P.; Hase, W. L. Born-Oppenheimer direct dynamics classical trajectory simulations. In *Reviews in Computational Chemistry*; Lipkowitz, K. B., Larter, R., Cundari, T. R., Boyd, D. B., Eds.; Wiley-VCH, Inc: New York, 2003; Vol. 19, pp 79–146.
- (15) Schlegel, H. B. Ab initio molecular dynamics with Born-Oppenheimer and extended Lagrangian methods using atom centered basis functions. *Bull. Korean Chem. Soc.* **2003**, *24*, 837–842.
- (16) Bunker, D. L. Classical trajectory methods. *Meth. Comput. Phys.* **1971**, *10*, 287.
- (17) Press, W. H. *Numerical Recipes in FORTRAN: The Art of Scientific Computing*, 2nd ed.; Cambridge University Press: Cambridge, England, 1992; pp xxvi, 963.
- (18) Helgaker, T.; Uggerud, E.; Jensen, H. J. A. Integration of the classical equations of motion on ab initio molecular-potential energy surfaces using gradients and Hessians - application to translational energy-release upon fragmentation. *Chem. Phys. Lett.* **1990**, *173*, 145–150.
- (19) Chen, W.; Hase, W. L.; Schlegel, H. B. Ab-initio classical trajectory study of $\text{H}_2\text{CO} \rightarrow \text{H}_2 + \text{CO}$ dissociation. *Chem. Phys. Lett.* **1994**, *228*, 436–442.
- (20) Millam, J. M.; Bakken, V.; Chen, W.; Hase, W. L.; Schlegel, H. B. Ab initio classical trajectories on the Born-Oppenheimer surface: Hessian-based integrators using fifth-order polynomial and rational function fits. *J. Chem. Phys.* **1999**, *111*, 3800–3805.
- (21) Bakken, V.; Millam, J. M.; Schlegel, H. B. Ab initio classical trajectories on the Born-Oppenheimer surface: Updating methods for Hessian-based integrators. *J. Chem. Phys.* **1999**, *111*, 8773–8777.
- (22) Wu, H.; Rahman, M.; Wang, J.; Louderaj, U.; Hase, W. L.; Zhuang, Y. Higher-accuracy schemes for approximating the Hessian from electronic structure calculations in chemical dynamics simulations. *J. Chem. Phys.* **2010**, *133*, 074101.
- (23) Lee, S. K.; Li, W.; Schlegel, H. B. HCO^+ dissociation in a strong laser field: An ab initio classical trajectory study. *Chem. Phys. Lett.* **2012**, *536*, 14–18.
- (24) Lancaster, P.; Salkauskas, K. *Curve and Surface Fitting, An Introduction*; Academic: London, 1986.
- (25) Ischtwan, J.; Collins, M. A. Molecular-potential energy surfaces by interpolation. *J. Chem. Phys.* **1994**, *100*, 8080–8088.
- (26) Bettens, R. P. A.; Collins, M. A. Learning to interpolate molecular potential energy surfaces with confidence: A Bayesian approach. *J. Chem. Phys.* **1999**, *111*, 816–826.
- (27) Hratchian, H. P.; Schlegel, H. B. Accurate reaction paths using a Hessian based predictor-corrector integrator. *J. Chem. Phys.* **2004**, *120*, 9918–9924.
- (28) Hratchian, H. P.; Schlegel, H. B. Using Hessian updating to increase the efficiency of a Hessian based predictor-corrector reaction path following method. *J. Chem. Theory Comput.* **2005**, *1*, 61–69.
- (29) Hratchian, H. P.; Kraka, E. Improved predictor-corrector integrators for evaluating reaction path curvature. *J. Chem. Theory Comput.* **2013**, *9*, 1481–1488.
- (30) Bofill, J. M. Updated hessian matrix and the restricted step method for locating transition structures. *J. Comput. Chem.* **1994**, *15*, 1–11.
- (31) Bofill, J. M. Remarks on the updated Hessian matrix methods. *Int. J. Quantum Chem.* **2003**, *94*, 324–332.
- (32) Frisch, M. J.; Trucks, G. W.; Schlegel, H. B.; Scuseria, G. E.; Robb, M. A.; Cheeseman, J. R.; Scalmani, G.; Barone, V.; Mennucci, B.; Petersson, G. A.; Nakatsuji, H.; Caricato, M.; Li, X.; Hratchian, H. P.; Izmaylov, A. F.; Bloino, J.; Zheng, G.; Sonnenberg, J. L.; Hada, M.; Ehara, M.; Toyota, K.; Fukuda, R.; Hasegawa, J.; Ishida, M.; Nakajima, T.; Honda, Y.; Kitao, O.; Nakai, H.; Vreven, T.; Montgomery, J. A., Jr.; Peralta, J. E.; Ogliaro, F.; Bearpark, M.; Heyd, J. J.; Brothers, E.; Kudin, K. N.; Staroverov, V. N.; Kobayashi, R.; Normand, J.; Raghavachari, K.; Rendell, A.; Burant, J. C.; Iyengar, S. S.; Tomasi, J.; Cossi, M.; Rega, N.; Millam, J. M.; Klene, M.; Knox, J. E.; Cross, J. B.; Bakken, V.;

Adamo, C.; Jaramillo, J.; Gomperts, R.; Stratmann, R. E.; Yazyev, O.; Austin, A. J.; Cammi, R.; Pomelli, C.; Ochterski, J. W.; Salvador, P.; Dannenberg, J. J.; Dapprich, S.; Parandekar, P. V.; Mayhall, N. J.; Daniels, A. D.; Farkas, O.; Foresman, J. B.; Ortiz, J. V.; Cioslowski, J.; Fox, D. J. *Gaussian Development Version*, Revision H; Gaussian, Inc.: Wallingford, CT, 2009.

(33) Psciuk, B. T.; Tao, P.; Schlegel, H. B. Ab initio classical trajectory study of the fragmentation of C₃H₄ dications on the singlet and triplet surfaces. *J. Phys. Chem. A* **2010**, *114*, 7653–7660.

(34) Mebel, A. M.; Bandrauk, A. D. Theoretical study of unimolecular decomposition of allene cations. *J. Chem. Phys.* **2008**, *129*, 224311.